Similarity index for seismic data sets using adaptive curvelets

Hasan Al-Marzouqi and Ghassan AlRegib
Center for Energy and Geo Processing (CeGP)
Georgia Institute of Technology

SUMMARY

In this paper, we propose a distance measure to evaluate visual similarity between two images. The algorithm searches for adaptive curvelet parameters that better represent a reference image. Next, the distance between the reference image and other images is computed as a weighted sum of distances between histograms of adaptive curvelet coefficients. The algorithm is tested on a data set of exemplary seismic activities. The developed measure is shown to be effective in extracting correct matches from the data set.

INTRODUCTION

In several technical fields, the size of data sets have increased considerably over the recent years because of various reasons including the advancement in sensing technologies. This has introduced new challenges to several applications that process such data. Examples include retrieval, clustering, and quality assessment. In all such applications, there is a need to use a similarity index that provides a quantified comparison between two data sets or signals. Such similarity index is required to be computationally efficient and insensitive to certain variation in the data such as rotation or linear translations.

Seismic data is complex and large in nature. There has been accumulation of huge seismic data for several decades. Some of these data sets have been investigated further with physical attributes and well logging. When a new survey data is available, it is useful to compare the new data to the old reservoir of data sets and find similar attributes. This will guide processing and interpretation stages with more informative assumptions. This comparison process could be performed on the raw pre-stack data, on the post-stack data, or on the migrated data. Although the literature focuses on developing advanced clustering, attributes recognition techniques, and other methods, it lacks rigorous investigation of the primary and common factor among all these methods, a meaningful similarity index.

Several attempts to develop a similarity index for seismic data sets have been proposed in the literature. The authors in Vyas and Sharma (2013) showed that the signal-to-noise ratio can be enhanced by only stacking those volumes that are similar to each other. Although the authors proposed the zero-lag correlation coefficient as a basic similarity measure, they have shown that considerable gains are obtained with such a simple similarity index. Another key trial at developing a similarity index for curve-based data sets such as seismic data sets is presented in Chiodi et al. (2013). The authors looked for simple transformation of waves, like the linear one, in order to measure similarity with the template, reference wave. The distance between a given wave **x** and the reference wave **C** is computed by

$$\tilde{\delta}(x,C) = \min_{a_s,b_s} \delta(\tilde{x},C), \tag{1}$$

where vector $s = 1,...,d$ indexes $\tilde{x}$ elements obtained through a linear wrapping defined by $h_s = a_s + b_s t$. Furthermore, Clustering is used as the application to the proposed similarity index where equation (1) is used to cluster curves into different partitions. The authors proposed a clustering algorithm that resembles the k-means method. Lee et al. (2009) used a similarity index that is based on principal component analysis (PCA) where the singular values (or the positive square root of the eignvalues of the covariance matrix containing the seismic data sets) are computed for both data sets. The proposed similarity index is given as the ratio between the largest eignvalue and the sum of the largest p eignvlaues. The authors tested the proposed similarity index on data sets used to model the sea bed in the Suyong Bay in South Korea. The computed similarity index values gave valuable information on areas with similar structure.

In this paper, we propose a similarity index for migrated seismic data sets. The proposed measure is based on the curves structure within the data set. We first compute the adaptive curvelet transform on the two 2D seismic sections we want to compare. Then, we process the curvelet-domain content and quantify the difference between wedges of the two 2D seismic sections. In the next section, we will present an overview of the adaptive curvelet transform. This will be followed by technical details of our approach and experimental results.

ADAPTIVE CURVELET TRANSFORM

The curvelet transform (Candes et al. (2006)) provides an efficient representation of directional features. It works by dividing the spatial content of images into different frequency bands representing unique scale and directional features. It has shown performance advantages in seismic denoising (Oueity et al. (2009)), multiple suppression (Herrmann et al. (2004)), compressed sensing retrieval (Herrmann et al. (2012)), and seismic imaging (Douma and de Hoop (2007)).

Curvelet coefficients are generated using the 2D fast Fourier transform (FFT). FFT is first applied to an image. Next, the 2D FFT plane is divided into different scales. The number of scales depend on the size of the image and is given by

$$J = \lceil \log_2(\min(N_1,N_2) - 3) \rceil, \tag{2}$$

where $\lceil * \rceil$ is the ceiling function, and N_1 and N_2 are the number of vertical and horizontal image pixels respectively. Scale locations, which we define as coordinates of the FFT plane

DOI http://dx.doi.org/10.1190/segam2014-1228.1

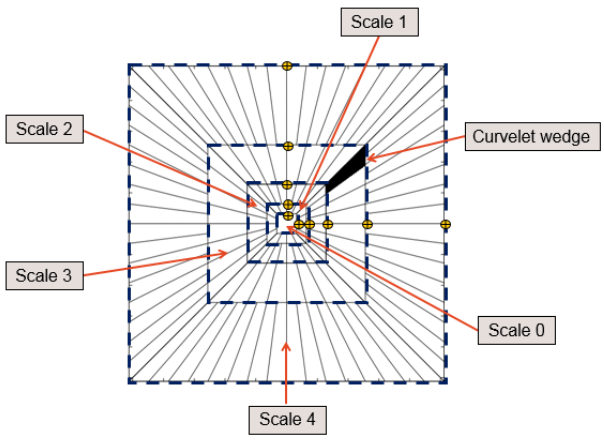

Figure 1: Default curvelet tiling. 5-scale decomposition is shown. Each scale is divided into $16 \times 2^{\lceil (j-1)/2 \rceil}$ wedges, where j is the scale number. Scale locations are denoted by yellow markers.

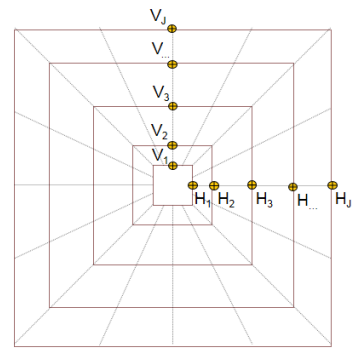

Figure 2: Vertical and horizontal scale locations.

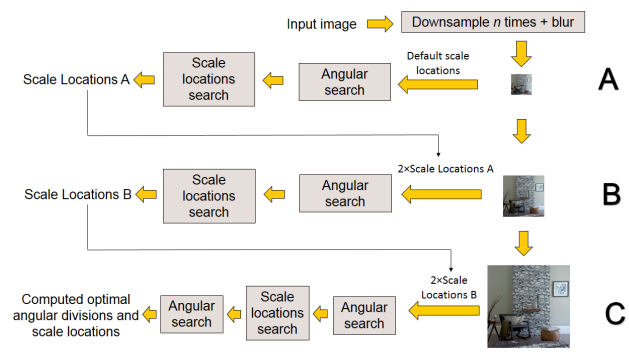

Figure 3: Flow diagram of the global optimization algorithm.

that determine the outer boundary of each scale, are determined in a dyadic manner. Each curvelet scale is further divided into a number of different directional wedges as shown in Figure 1. Curvelet coefficients are generated by taking the IFFT's of these wedges.

Adaptive curvelets improve default curvelets performance by adapting the frequency divisions to better represent the content of a given image. In adaptive curvelets, the frequency tiling that provides maximal improvements in cost function values is considered optimal (Al-Marzouqi and AlRegib (2013a)). Adaptation parameters include the number of angular divisions per scale/quadrant pair and scale locations. In seismic data, the optimal choice for these parameters is found using an optimization algorithm maximizing the coefficient of variation C_v of curvelet coefficients magnitude, where $C_v = \sigma/\mu$ (Al-Marzouqi and AlRegib (2013b)). Angular decompositions are optimized separately from scale location. A multi-resolution global optimization algorithm combining angular optimization and scale locations search is used to find the optimal adaptive curvelet parameters.

Optimal Number of Angular Divisions per Scale/Quadrant
Optimizing the number of angular divisions is performed using exhaustive search. The tested parameters are chosen from the following sequence $\{4, 8, 12, 16, 20, 24\}$. The divisions are uniformly distributed in each scale/quadrant pair. Recalling FFT's symmetry for real data the number of parameters to optimize is $2\times(J\text{-}1)$ for real data, and is equal to $4\times(J\text{-}1)$ for the case of complex input data. The distribution of angular decompositions that generates the maximum C_v value is considered optimal.

Optimal Scale Locations
Derivative-free optimization methods are used to find the optimal scale locations. Such methods start at an initial point x_0, evaluate the cost function at a selected mesh of points in the neighborhood of x_0, and define the point in the mesh with the minimum function value as the new x_0. Next, the algorithm iterates until a specified convergence criteria is met. The Nelder-Mead simplex search method (Conn et al. (2009); Nelder and Mead (1965)) is one of the popular methods for generating such a mesh. It has been used extensively in a variety of application areas. It is used in this work to find the optimal scale locations. Given a specific angular distribution the scale locations search algorithm finds vectors $\mathbf{H}$ and $\mathbf{V}$, where $\mathbf{V} = \{V_1, V_2, ..., V_J\}$ are the coordinates of vertical scale locations, and $\mathbf{H} = \{H_1, H_2, ..., H_J\}$ are the horizontal scale locations (Figure 2).

Global Optimization
In this part, we introduce the global optimization algorithm that combines the two previous adaptations. The algorithm uses a multi-resolution search strategy. This helps in avoiding convergence to local minima, and reduces the computational cost of the algorithm. Optimization is done in a hierarchical manner consisting of n iterations. In each iteration, optimal scale and angular locations are found for a downsampled smoothed version of the input image. The flow of this algorithm is illustrated in Figure 3.

The algorithm starts with downsampling the original image $n-1$ times by a factor of two. The image is also smoothed by a Gaussian filter. The optimal angular decomposition is found using dyadic scale locations and the optimal number of scales computed using equation (2). The angular decomposi-

DOI http://dx.doi.org/10.1190/segam2014-1228.1

tions found and the dyadic scale locations are used as initial points for the scale locations search algorithm. Next, the value of n is decremented by one and a new loop starts. Initial values for scale locations will be the scale locations computed in the previous iteration after being re-scaled to the new image coordinates. After n iterations, once the scale locations search algorithm converges to a minimum, the angular decomposition algorithm is run to search for the optimal angular decomposition at the calculated scale locations. Finally, the algorithm terminates returning the determined optimal scale and angular decompositions.

SIMILARITY INDEX

Computing the similarity index begins by finding the optimal curvelet representing one of the images to be compared. We refer to this image as the reference image. Maximizing the coefficient of variation is the cost function used to find the optimal frequency domain tiling. Next, the computed adaptive curvelet is applied to the reference and target images. Let $H_{j,l}$ be a histogram of curvelet of coefficients representing a curvelet wedge at scale j and location l. Define

$$\widehat{H}_{j,l} = \mathbf{v}_{j,l} \cdot H_{j,l}, \tag{3}$$

where $v_{j,l}$ is a vector of $H_{j,l}$ center bin values. Twenty histogram bins were used in this study. We define the distance between images A and B to be a weighted sum of distances between $\widehat{H}_{j,l}$ vectors representing A and B. The distance is given by:

$$D(A,B) = \frac{1}{N}\sum_{j=1}^{J}\sum_{l=1}^{L} w_{j,l}\|\widehat{H}^A_{j,l} - \widehat{H}^B_{j,l}\|_1, \tag{4}$$

where $\|x\|_1$ is the l_1 norm of x, $w_{j,l}$ is the ratio between curvelet coefficients energy at wedge $\{j,l\}$ and the total energy in images A and B. It is described by the following equation:

$$w_{j,l} = \frac{\sum_{\forall m_1,m_2} |c^A_{j,l}[m_1,m_2]|^2 + \sum_{\forall m_1,m_2} |c^B_{j,l}[m_1,m_2]|^2}{\sum_{\forall n_1,n_2} A^2[n_1,n_2] + \sum_{\forall n_1,n_2} B^2[n_1,n_2]}, \tag{5}$$

where m_1 and m_2 index curvelet coefficients at wedge $\{j,l\}$. n_1 and n_2 are image coordinates. In Equation 4, N is a normalization factor and is chosen to be

$$N = max(\|C^A\|_2, \|C^B\|_2), \tag{6}$$

where C^A and C^B are the curvelet coefficients representing images A and B respectively. The distance measure can be generalized to include weights for different curvelet scales and directions. Using such weights is useful for detecting activities at certain frequency ranges (*i.e.* emphasizing coarser or finer features) or directions. A generalized form of the distance measure is given by

$$D(A,B) = \frac{1}{N}\sum_{j=1}^{J} w_s \sum_{l=1}^{L} w_d w_{j,l}\|\widehat{H}^A_{j,l} - \widehat{H}^B_{j,l}\|_1, \tag{7}$$

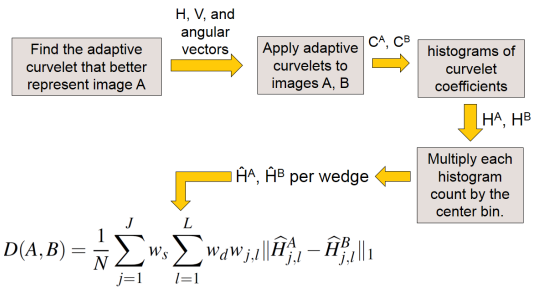

$$D(A,B) = \frac{1}{N}\sum_{j=1}^{J} w_s \sum_{l=1}^{L} w_d w_{j,l}\|\widehat{H}^A_{j,l} - \widehat{H}^B_{j,l}\|_1$$

Figure 4: Computing the distance measure.

Figure 5: Distance measure D and blurring effects: (a) `cameraman` image (b) Blurred with averaging filter of size five $D = 26.0$ (c) Blurred with averaging filter of size ten $D = 51.9$

where w_s is a vector of weights given to different curvelet scales and w_d is a vector of weights given to curvelet directional wedges. The flow of the algorithm is summarized in Figure 4.

The similarity index between two identical images is equal to zero. Ideally, the value of the index increases as images vary in structure. Examples of similarity index values are shown in Figure 5. The distance measure is computed for an image that is blurred with averaging filters of sizes 5×5 and 10×10.

CHARACTERIZING SEISMIC DATA SETS USING THE SIMILARITY INDEX

The similarity index was tested on 12 seismic data sets of size 100×200 pixels. The data are extracted from Netherlands offshore F3 block acquired in the North Sea (Opendtect (2014)). The extracted data set resembles four different seismic activities. Figure 6 shows the images used in this study. We considered the following seismic activities:

Fault Data sets with faults

Horizontal Data sets with obvious horizons

Dome Data sets with salt dome shapes and alike

Clear Data sets with none of the above activities

A single image from each category was chosen as the reference image. The remaining images were used as target images. Weight vectors w_d and w_s were set to one, except for the dome shaped images. In dome shaped images, the similarity measure was computed using only the outer two curvelet

DOI http://dx.doi.org/10.1190/segam2014-1228.1

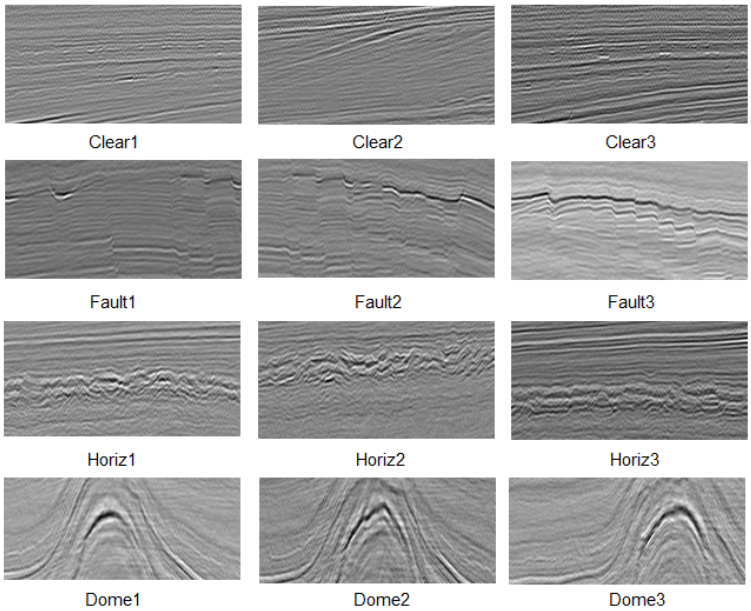

Figure 6: Seismic images used in this study.

	Clear2	Clear3	Fault2	Fault3	Horiz2	Horiz3	Dome2	Dome3
Clear1	**2.28**	**2.54**	4.16	5.64	2.75	2.81	5.03	7.30
Fault1	5.10	6.34	**3.12**	**3.25**	5.68	5.11	6.66	5.68
Horiz1	3.30	4.03	4.47	5.70	**2.31**	**2.86**	4.65	7.25
Dome1	1.82	2.92	0.85	0.67	0.76	1.14	**0.35**	**0.38**

Table 1: Similarity index values computed using adaptive curvelet transform.

	Clear2	Clear3	Fault2	Fault3	Horiz2	Horiz3	Dome2	Dome3
Clear1	5.44	**4.16**	4.19	**3.96**	4.38	5.69	5.31	5.55
Fault1	4.88	4.91	**3.01**	**3.00**	3.33	3.50	3.50	3.50
Horiz1	3.57	3.72	**2.35**	2.73	**2.12**	2.88	2.96	2.98
Dome1	2.71	3.90	2.04	1.83	1.46	1.75	**0.89**	**0.79**

Table 2: Similarity index values computed using the default curvelet transform.

scales (*i.e.* $w_s = [0\,0\,1\,1]$). Results are shown in Table 1. Lower values of D indicate higher similarity levels between the reference and target images. The algorithm succeeds in matching reference images with images in the correct category. The displacements of dome shaped features did not affect classification results. Similarly, the algorithm was invariant to displacements and small orientation changes in horizontal activity images. The algorithm was also robust to changes in the number of faults. Repeating the same experiment with interchanged reference and target images generated a number of mismatches. The presented similarity index is not invariant to changes in scale and orientation. A rotation and scale invariant version of the index is under development.

The same experiment was repeated using default curvelets instead of adaptive curvelets and the results are shown in Table 2. Default curvelet results generate two wrong matches for `Clear1` and `Horiz1` images. `Clear1` image are mistakenly reported to be more similar to fault images than the corresponding `Clear2` image. Using default curvelets, `Horiz1` image are also mistakenly reported to be closer to fault images than the corresponding `Horiz3` image.

CONCLUSIONS

A distance measure between seismic images was presented in this paper. The measure assess the visual similarity between two images using the distribution of adaptive curvelet coefficients. In our experiments, it was shown to be successful in identifying seismic events. In the future, we plan to extend the experimental analysis to include larger seismic data sets. We also plan to apply the algorithm to texture classification problems.

DOI http://dx.doi.org/10.1190/segam2014-1228.1

http://dx.doi.org/10.1190/segam2014-1228.1

EDITED REFERENCES

Note: This reference list is a copy-edited version of the reference list submitted by the author. Reference lists for the 2014 SEG Technical Program Expanded Abstracts have been copy edited so that references provided with the online metadata for each paper will achieve a high degree of linking to cited sources that appear on the Web.

REFERENCES

Al-Marzouqi, H., and G. AlRegib, 2013a, Searching for the optimal curvelet tiling: International Conference on Acoustics, Speech, and Signal Processing, IEEE, 1626–1630.

Al-Marzouqi, H., and G. AlRegib, 2013b, Using the coefficient of variation to improve the sparsity of seismic data: Presented at the First IEEE Global Conference on Signal and Information Processing.

Candès, E., L. Demanet, D. Donoho, and L. Ying, 2006, Fast-discrete curvelet transforms: Multiscale Modeling & Simulation, **5**, no. 3, 861–899, http://dx.doi.org/10.1137/05064182X.

Chiodi, M., and G. Adelfio, A. DAlessandro, and D. Luzio, 2013, Clustering and registration of multidimensional functional data, *in* Statistical models for data analysis: Springer International Publishing, Studies in Classification, Data Analysis, and Knowledge Organization, 89–97.

Conn, A. A. R., K. Scheinberg, and L. N. Vicente, 2009, Introduction to derivative-free optimization: SIAM, 8.

Douma, H., and M. de Hoop, 2007, Leading-order seismic imaging using curvelets: Geophysics, **72**, no. 6, S231–S248, http://dx.doi.org/10.1190/1.2785047.

Herrmann, F., M. Friedlander, and O. Yilmaz, 2012, Fighting the curse of dimensionality: Compressive sensing in exploration seismology: Signal Processing Magazine, IEEE, **29**, no. 3, 88–100, http://dx.doi.org/10.1109/MSP.2012.2185859.

Herrmann, F. J., and E. Verschuur, 2004, Curvelet-domain multiple elimination with sparseness constraints: 74th Annual International Meeting, SEG, Expanded Abstracts, 1333–1336.

Lee, G. H., H. J. Kim, D. C. Kim, B. Y. Yi, S. M. Nam, B. K. Khim, and M. S. Lim, 2009, The acoustic diversity of the seabed based on the similarity index computed from chirp seismic data.: ICES Journal of Marine Science/Journal du Conseil, **66**, 227 – 236.

Nelder, J. A., and R. Mead, 1965, A simplex method for function minimization: The Computer Journal, **7**, no. 4, 308–313, http://dx.doi.org/10.1093/comjnl/7.4.308.

Opendtect, 2014, https://opendtect.org/osr/ pmwiki.php/Main/HomePage.

Oueity, J., V. Kumar, R. Clowes, and F. Herrmann, 2009, Curvelet denoising: Application to crustal reflection data: Frontiers & Innovation, CSPG.

Vyas, M., and A. Sharma, 2013, Systems and methods for optimal stacking of seismic data: U. S. Patent App. 13/855,783.